particularly when term approaches. The imbalance in T-cell immunity (Th1/Th2) has been proposed to be implicated in the progression of chronic HEV infection in immunocompromised pigs (*7*). This imbalance may explain the absence of cytolysis during pregnancy and the increased viral load observed despite discontinuation of infliximab. Conversely, after delivery, restoration of cellular immunity is commonly observed (*11*) and may have contributed to efficient clearance of the virus by hepatic cytolysis along with the reduced immunosuppression resulting from infliximab discontinuation. Despite reintroduction of infliximab when HEV RNA was still detectable, we observed spontaneous resolution of chronic hepatitis E, although immunosuppressive treatment at that time was identical to that previously implicated in the chronicity of infection.

The risk for HEV vertical transmission seems dependent on viral load (*12*). In a model of HEV infection in pregnant rabbits, Xia et al. reported severe outcomes and a high level of transmission to offspring (*13*). In the case we report, despite high viral loads in the mother's plasma throughout pregnancy, we found no HEV RNA in the newborn's plasma. Of note, although mothers in the rabbit model were negative for HEV IgG throughout pregnancy, in the case we report, the mother was IgG positive before pregnancy, which may have helped protect the fetus from infection, although this protective role is inconsistent in previous reports of HEV genotype 3 (HEV3) infection of humans (*2–4*). Furthermore, despite a high sequence similarity to HEV3, rabbit HEV cross-species infections are restricted to nonhuman primates, and pathogenesis may differ from that of HEV3. In conclusion, our results and those reported by Mallet et al. (*5*) indicate that chronic HEV3 infection in pregnant women might resolve after pregnancy.

About the Author

Dr. Charre is a microbiologist in the virology laboratory of the Institute of Infectious Agents, Hospices Civils de Lyon, Lyon, France. Her research and teaching interests focus on viral hepatitis and human immunodeficiency virus.

References

1. Kamar N, Izopet J, Pavio N, Aggarwal R, Labrique A, Wedemeyer H, et al. Hepatitis E virus infection. Nat Rev Dis Primers. 2017;3:17086. http://dx.doi.org/10.1038/nrdp.2017.86
2. Andersson MI, Hughes J, Gordon FH, Ijaz S, Donati M. Of pigs and pregnancy. Lancet. 2008;372:1192. http://dx.doi.org/10.1016/S0140-6736(08)61486-5
3. Anty R, Ollier L, Péron JM, Nicand E, Cannavo I, Bongain A, et al. First case report of an acute genotype 3 hepatitis E infected pregnant woman living in South-Eastern France. J Clin Virol. 2012;54:76–8. http://dx.doi.org/10.1016/j.jcv.2012.01.016
4. Tabatabai J, Wenzel JJ, Soboletzki M, Flux C, Navid MH, Schnitzler P. First case report of an acute hepatitis E subgenotype 3c infection during pregnancy in Germany. J Clin Virol. 2014;61:170–2. http://dx.doi.org/10.1016/j.jcv.2014.06.008
5. Mallet V, Le Mener S, Roque-Afonso A-M, Tsatsaris V, Mamzer M-F. Chronic hepatitis E infection cured by pregnancy. J Clin Virol. 2013;58:745–7. http://dx.doi.org/10.1016/j.jcv.2013.09.023
6. Grewal P, Kamili S, Motamed D. Chronic hepatitis E in an immunocompetent patient: a case report. Hepatology. 2014;59:347–8. http://dx.doi.org/10.1002/hep.26636
7. Cao D, Cao QM, Subramaniam S, Yugo DM, Heffron CL, Rogers AJ, et al. Pig model mimicking chronic hepatitis E virus infection in immunocompromised patients to assess immune correlates during chronicity. Proc Natl Acad Sci U S A. 2017;114:6914–23. http://dx.doi.org/10.1073/pnas.1705446114
8. Mansuy JM, Gallian P, Dimeglio C, Saune K, Arnaud C, Pelletier B, et al. A nationwide survey of hepatitis E viral infection in French blood donors. Hepatol Baltim Md. 2016;63:1145–54.
9. Dalton HR, Pas SD, Madden RG, van der Eijk AA. Hepatitis E virus: current concepts and future perspectives. Curr Infect Dis Rep. 2014;16:399.
10. Sehgal R, Patra S, David P, Vyas A, Khanam A, Hissar S, et al. Impaired monocyte-macrophage functions and defective Toll-like receptor signaling in hepatitis E virus–infected pregnant women with acute liver failure. Hepatology. 2015;62:1683–96. http://dx.doi.org/10.1002/hep.28143
11. Elenkov IJ, Wilder RL, Bakalov VK, Link AA, Dimitrov MA, Fisher S, et al. IL-12, TNF-α, and hormonal changes during late pregnancy and early postpartum: implications for autoimmune disease activity during these times. J Clin Endocrinol Metab. 2001;86:4933–8.
12. Sharma S, Kumar A, Kar P, Agarwal S, Ramji S, Husain SA, et al. Risk factors for vertical transmission of hepatitis E virus infection. J Viral Hepat. 2017;24:1067–75. http://dx.doi.org/10.1111/jvh.12730
13. Xia J, Liu L, Wang L, Zhang Y, Zeng H, Liu P, et al. Experimental infection of pregnant rabbits with hepatitis E virus demonstrating high mortality and vertical transmission. J Viral Hepat. 2015;22:850–7. http://dx.doi.org/10.1111/jvh.12406

Address for correspondence: Caroline Charre, Laboratoire de Virologie, Hôpital de la Croix-Rousse, Hospices Civils de Lyon, 103 Grande de la Croix Rousse, 69004 Lyon, France; email: caroline.charre@chu-lyon.fr

Multiple Introductions of Influenza A(H5N8) Virus into Poultry, Egypt, 2017

Ahmed H. Salaheldin, Hatem Salah Abd El-Hamid, Ahmed R. Elbestawy, Jutta Veits, Hafez M. Hafez, Thomas C. Mettenleiter, Elsayed M. Abdelwhab

Author affiliations: Alexandria University, Al Buhayrah, Egypt (A.H. Salaheldin); Friedrich-Loeffler-Institut, Insel Riems-Greifswald, Germany (A.H. Salaheldin, J. Veits, T.C. Mettenleiter,

E.M. Abdelwhab); Freie-Universität-Berlin, Berlin, Germany (A.H. Salaheldin, H.M. Hafez); Damanhour University, Damanhour, Egypt (H.S. Abd El-Hamid, A.R. Elbestawy)

DOI: https://doi.org/10.3201/eid2405.171935

After high mortality rates among commercial poultry were reported in Egypt in 2017, we genetically characterized 4 distinct influenza A(H5N8) viruses isolated from poultry. Full-genome analysis indicated separate introductions of H5N8 clade 2.3.4.4 reassortants from Europe and Asia into Egypt, which poses a serious threat for poultry and humans.

In Egypt, highly pathogenic avian influenza A(H5N1) clade 2.2.1 virus was introduced to poultry via migratory birds in late 2005 (*1*) and is now endemic among poultry in Egypt (*2*). Also in Egypt, the number of H5N1 infections in humans is the highest in the world, and low pathogenicity influenza A(H9N2) virus is widespread among poultry and has infected humans (*2*). Despite extensive vaccination, H5N1 and H9N2 viruses are co-circulating and frequently reported (*2*). In 2014, highly pathogenic avian influenza A(H5N8) virus clade 2.3.4.4 was isolated, mostly from wild birds, in several Eurasian countries and was transmitted to North America. However, in 2016 and 2017, an unprecedented epidemic was reported in Asia, Africa, and Europe (*3*). In Egypt, during November 30–December 8, 2016, a total of 3 H5N8 viruses were isolated from common coot (*Fulica atra*) (*4*) and green-winged teal (*Anas carolinensis*) (*5*). To provide data on the spread of the virus in poultry, we genetically characterized 4 distinct H5N8 viruses isolated from commercial poultry in Egypt in 2017.

During February–May 2017, a high mortality rate was observed for 48 poultry flocks in the Nile Delta, Egypt. Up to 20 tracheal and cloacal swab samples were collected from each flock for initial diagnosis by reverse transcription PCR and virus isolation at the Faculty of Veterinary Medicine, Damanhour University (Damanhour, Egypt). Results were positive for H5N8 virus in samples for 4 flocks not vaccinated for H5 in 3 governorates (Figure). Sudden deaths also occurred in 3 broiler chicken flocks (Ck12, Ck15, Ck21) and 1 duck flock (Dk18); mortality rates were 29%–52% (online Technical Appendix 1 Table 1, https://wwwnc.cdc.gov/EID/article/24/5/17-1935-Techapp1.pdf). No epidemiologic links between farms were observed.

Positive samples were spotted onto FTA cards (*6*) and submitted to Friedrich-Loeffler-Institut (Insel Riems-Greifswald, Germany), where H5N8 virus was confirmed

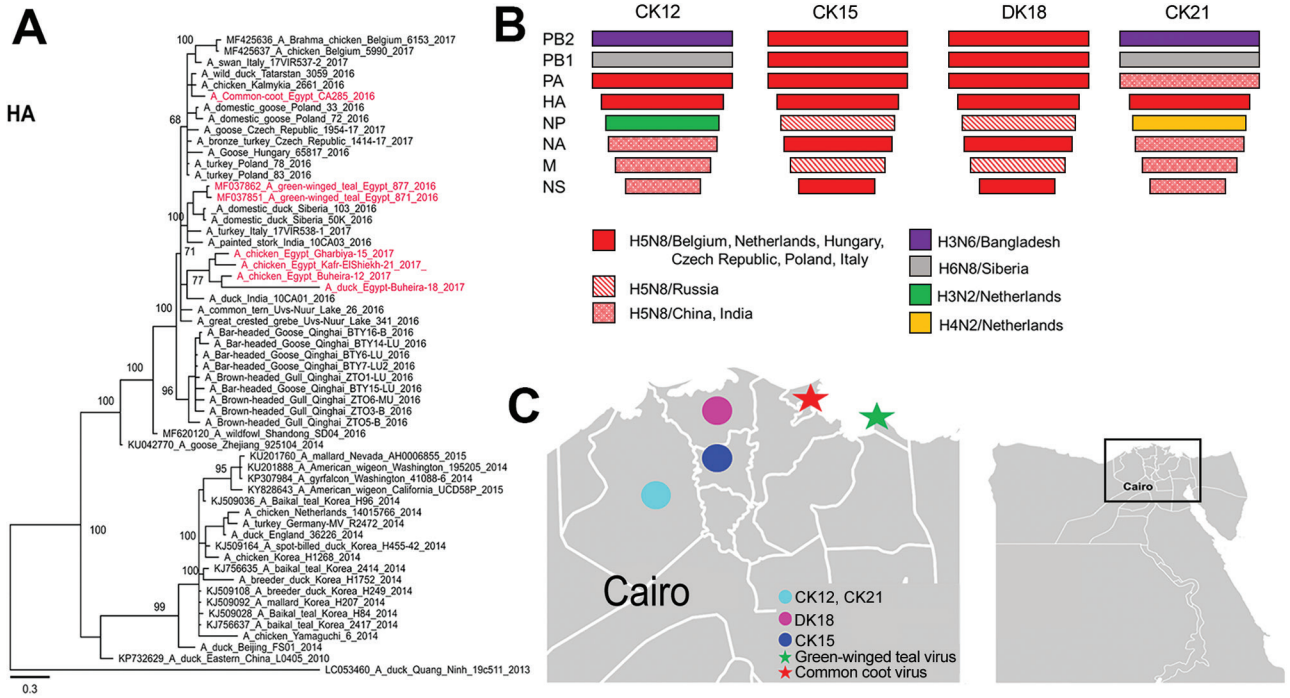

Figure. Characterization of highly pathogenic avian influenza A(H5N8) viruses of clade 2.3.4.4 from Egypt, 2017. A) Phylogenetic relatedness of the HA gene and schematic representation of potential precursors of different H5N8 viruses. The maximum-likelihood midpoint rooted tree was constructed by using MrBayes (http://mrbayes.sourceforge.net/). Gray indicates viruses from this study. Scale bar indicates nucleotide substitutions per site. B) Putative ancestors of the different gene segments of H5N8 viruses from Egypt characterized in this study compared with reference viruses. C) Governorates in Egypt where H5N8 viruses had been reported in domestic birds (circles) and where viruses in birds had been previously reported (stars). Inset shows study location in Egypt. Ck, chicken farm; Dk, duck farm; HA, hemagglutinin; M, matrix; NA, neuraminidase; NP, nucleocapsid protein; NS, nonstructural; PA, polymerase acidic; PB, polymerase basic.

by reverse transcription PCR and full-genome sequences (*7*) from 4 viruses (GISAID [https://www.gisaid.org/] accession nos. EPI1104268–EPI1104299) (online Technical Appendix 2, https://wwwnc.cdc.gov/EID/article/24/5/17-1935-Techapp2.pdf). We retrieved sequences with high similarity and all H5N8 virus sequences from GISAID and GenBank and aligned them by Multiple Alignment using Fast Fourier Transform (https://mafft.cbrc.jp/alignment/server/index.html). The most highly related viruses are summarized in online Technical Appendix 1 Table 2. We calculated sequence identity matrices in Geneious (https://www.geneious.com/) (online Technical Appendix 1 Figure 1) and studied phylogenetic relatedness to H5N8 virus isolated in Eurasia and in Egypt by using IQtree (http://www.iqtree.org/). Representative viruses were selected for generation of maximum-likelihood midpoint rooted trees by MrBayes (http://mrbayes.sourceforge.net/) using a best-fit model (GTR+G) (*8*) and were further edited by using FigTree (http://tree.bio.ed.ac.uk/software/figtree/) and Inkscape (https://inkscape.org/en/).

The hemagglutinin (HA) and neuraminidase (NA) genes of the 4 viruses shared 95.8%–99.2% nt and 93.1%–99.4% aa identity and shared 96.5%–99.2% nt and 94.2%–99.7% aa identity with viruses from wild birds in Egypt (*4*,*5*). Other segments showed 92.6%–99.6% nt and 96%–99.7% aa identity, where the polymerase acidic (PA) genes and proteins of viruses from Dk18 showed the lowest similarity to those of other viruses (online Technical Appendix 1 Figure 1).

All viruses possess the polybasic HA cleavage site PLREKRRKR/G and contain mammal-adaptation and virulence markers (*9*) in polymerase basic (PB) 2 (T63I, L89V, G309D, T339K, Q368R, H447Q, R477G), PB1 (A3V, L13P, K328N, S375N, H436Y, M677T), PA (A515T), HA (T156A, A263T; H5 numbering), matrix (M) 1 (N30D, T215A), and nonstructural (NS) 1 (P42S, T127N, V149A) proteins. Therefore, protection of humans and risk assessment of bird-to-human transmission is crucial. The NS1 protein from viruses from Ck15 and Ck18 is 217 aa long because of truncation in the C-terminus, whereas NS1 of the other H5N8 viruses from Egypt are 230 aa long. BLAST (http://blast.ncbi.nlm.nih.gov/Blast.cgi) analysis indicated that these 4 viruses differ from viruses isolated from birds in live bird markets in Egypt in 2016 (*4*,*5*). Gene segments were closely related to viruses isolated from wild birds, poultry, and zoo birds in Europe (including Belgium, Czech Republic, the Netherlands, Poland, Hungary), Russia, and Asia (including Bangladesh, China, India) (Figure; online Technical Appendix 1 Figures 2, 3).

HA of the 4 H5N8 viruses in this study clustered in 1 distinct branch (Figure), and NA clustered in 2 phylogroups (online Technical Appendix 1 Figure 2). The PB2, nucleoprotein, M, and NS genes of viruses from Ck12 and Ck21 (from chickens in the same governorate, February and May 2017) clustered together, and the same genes from viruses from Dk18 and Ck15 (from ducks and chickens in 2 governorates) clustered in 2 distinct phylogenetic groups. However, viruses from Ck12 and Ck15 have similar but not identical PA gene segments (online Technical Appendix 1 Figure 3).

These data suggest 4 different introductions of H5N8 virus into poultry in Egypt, independent of viruses isolated from captive birds (*4*,*5*). Multiple separate introductions of H5N8 virus into Europe also occurred (*10*). Further studies are needed to identify the source(s) of introduction. The separate introductions of different reassortants of H5N8 clade 2.3.4.4 virus from Europe and Asia into Egypt indicate a serious threat for poultry and human health.

Acknowledgments

We acknowledge Günter Strebelow for his assistance with sequencing of viruses in this study, and we thank the colleagues and laboratories who submitted sequence data to GISAID.

A.H.S. is supported by internal funds from Friedrich-Loeffler-Institut, Federal Research Institute for Animal Health.

About the Author

Mr. Salaheldin is a doctoral student at the Institute of Poultry Diseases, Freie-Universität-Berlin. His primary research interests are molecular virology, vaccine development, and epidemiology of avian influenza viruses.

References

1. Saad MD, Ahmed LS, Gamal-Eldein MA, Fouda MK, Khalil F, Yingst SL, et al. Possible avian influenza (H5N1) from migratory bird, Egypt. Emerg Infect Dis. 2007;13:1120–1 http://dx.doi.org/10.3201/eid1307.061222
2. Abdelwhab EM, Hassan MK, Abdel-Moneim AS, Naguib MM, Mostafa A, Hussein IT, et al. Introduction and enzootic of A/H5N1 in Egypt: virus evolution, pathogenicity and vaccine efficacy ten years on. Infect Genet Evol. 2016;40:80–90. http://dx.doi.org/10.1016/j.meegid.2016.02.023
3. World Organisation for Animal Health. Update on avian influenza in animals (types H5 and H7): 2017 [cited 2017 Nov 10]. http://www.oie.int/animal-health-in-the-world/update-on-avian-influenza/
4. Selim AA, Erfan AM, Hagag N, Zanaty A, Samir AH, Samy M, et al. Highly pathogenic avian influenza virus (H5N8) clade 2.3.4.4 infection in migratory birds, Egypt. Emerg Infect Dis. 2017;23:1048–51. http://dx.doi.org/10.3201/eid2306.162056
5. Kandeil A, Kayed A, Moatasim Y, Webby RJ, McKenzie PP, Kayali G, et al. Genetic characterization of highly pathogenic avian influenza A H5N8 viruses isolated from wild birds in Egypt. J Gen Virol. 2017;98:1573–86. http://dx.doi.org/10.1099/jgv.0.000847
6. Abdelwhab EM, Lüschow D, Harder TC, Hafez HM. The use of FTA® filter papers for diagnosis of avian influenza virus. J Virol Methods. 2011;174:120–2. http://dx.doi.org/10.1016/j.jviromet.2011.03.017
7. Hoffmann E, Stech J, Guan Y, Webster RG, Perez DR. Universal primer set for the full-length amplification of all influenza A

viruses. Arch Virol. 2001;146:2275–89 https://doi.org/10.1007/s007050170002. http://dx.doi.org/10.1007/s007050170002
8. Milne I, Lindner D, Bayer M, Husmeier D, McGuire G, Marshall DF, et al. TOPALi v2: a rich graphical interface for evolutionary analyses of multiple alignments on HPC clusters and multi-core desktops. Bioinformatics. 2009;25:126–7. http://dx.doi.org/10.1093/bioinformatics/btn575
9. Mertens E, Dugan VG, Stockwell TB, Lindsay LL, Plancarte M, Boyce WM. Evaluation of phenotypic markers in full genome sequences of avian influenza isolates from California. Comp Immunol Microbiol Infect Dis. 2013;36:521–36. http://dx.doi.org/10.1016/j.cimid.2013.06.003
10. Fusaro A, Monne I, Mulatti P, Zecchin B, Bonfanti L, Ormelli S, et al. Genetic diversity of highly pathogenic avian influenza A(H5N8/H5N5) viruses in Italy, 2016–17. Emerg Infect Dis. 2017;23:1543–7. http://dx.doi.org/10.3201/eid2309.170539

Address for correspondence: Elsayed M. Abd El-Whab, Friedrich-Loeffler-Institut, Federal Research Institute for Animal Health, Suedufer 10, 17493 Insel Riems-Greifswald, Germany; email: sayed.abdel-whab@fli.de or sayedabdelwhab@yahoo.com

Fatal Tick-Borne Encephalitis Virus Infections Caused by Siberian and European Subtypes, Finland, 2015

Suvi Kuivanen, Teemu Smura, Kirsi Rantanen, Leena Kämppi, Jonas Kantonen, Mia Kero, Anu Jääskeläinen, Anne J. Jääskeläinen, Jussi Sane, Liisa Myllykangas, Anders Paetau, Olli Vapalahti

Author affiliations: University of Helsinki, Helsinki, Finland (S. Kuivanen, T. Smura, J. Kantonen, M. Kero, A. Jääskeläinen, L. Myllykangas, A. Paetau, O. Vapalahti); Helsinki University Hospital, Helsinki (K. Rantanen, L. Kämppi, A.J. Jääskeläinen, O. Vapalahti); National Institute for Health and Welfare, Helsinki (J. Sane)

DOI: https://doi.org/10.3201/eid2405.171986

In most locations except for Russia, tick-borne encephalitis is mainly caused by the European virus subtype. In 2015, fatal infections caused by European and Siberian tick-borne encephalitis virus subtypes in the same *Ixodes ricinus* tick focus in Finland raised concern over further spread of the Siberian subtype among widespread tick species.

The causative agent of tick-borne encephalitis (TBE), tick-borne encephalitis virus (TBEV), is endemic throughout Europe and Asia; ≈10,000 cases are reported annually (*1*). TBEV is an enveloped, positive-sense RNA virus in the family *Flaviviridae*, genus *Flavivirus* (*2*). The westernmost range of the Siberian subtype (TBEV-Sib) extends to Finland and the Baltics, where the European subtype (TBEV-Eur) also circulates. TBEV-Eur is the only subtype found in the rest of Europe (*3*).

In TBEV-infected patients, neurologic signs appear as the virus passes to the central nervous system; infection is manifested as meningitis, encephalitis, or meningoencephalitis. During 2010–2016, a total of 20 cases of TBE were reported from Kotka archipelago, Finland, a previous TBEV-Sib focus (*4*). We report 2 fatal TBEV infections acquired 1 month apart in patients on Kuutsalo Island, Kotka archipelago, in 2015.

Patient 1 was a previously healthy 36-year-old woman who had visited Kuutsalo 10 days before fever onset. A week later, she experienced sudden-onset headache, left arm numbness, and impaired vision. Head computed tomography results were unremarkable. Two days later, she experienced disorientation and right hemiparesis and was taken to a tertiary care center. Cerebrospinal fluid (CSF) test results showed pleocytosis. Magnetic resonance images indicated pathologically increased signal in cortical sulcus regions (Figure, panel A). Despite receipt of acyclovir, doxycycline, and ceftriaxone, her condition deteriorated rapidly. Head computed tomography showed cerebellar herniation; the patient had dilated pupils and no pain reaction. CSF and serum were positive for TBEV IgM but negative for TBEV RNA; hemagglutination inhibition results showed a low titer (20) of TBEV-specific antibodies in serum. The patient died 2 weeks after fever onset.

Gross postmortem examination showed widespread and severe signs of viral encephalitis: meningeal and perivascular inflammation, neuronophagy, microglial nodules, endothelial damage, and severe brain edema. The inflammation was evident from the spinal cord to the cerebellum and cortex (Figure, panel B). TBEV (RNA) was detected in brain and spleen (online Technical Appendix Figure 1, panel A, https://wwwnc.cdc.gov/EID/article/24/5/17-1986-Techapp1.pdf).

TBEV was isolated from the cerebellum in SK-N-SH neuroblastoma cells, and the whole genome for TBEV-Sib was obtained. A pool of TBEV-Sib–positive *Ixodes ricinus* ticks collected from the neighboring island in 2011 (*4*) was subjected to viral whole-genome sequencing. This virus and the virus from patient 1 had 3 nt differences resulting in 2 aa mutations, R868K (NS1) and V1452A (NS2B), and clustered together in the Baltic clade of TBEV-Sib (online Technical Appendix Figure 2).

Patient 2 was a 66-year-old man with hypertension, diabetes, and chronic lymphatic leukemia. He had frequently

Article DOI: https://doi.org/10.3201/eid2405.171935

Multiple Introductions of Influenza A(H5N8) Virus into Poultry, Egypt, 2017

Technical Appendix 1

Technical Appendix 1 Table 1. History of flocks infected with HPAIV H5N8 in 2017 characterized in this study

H5N8 Virus	Birds	Date	Governorate	No. birds	Age	Mortality
A/chicken/Egypt/Buheira-12/2017	Broilers	Mar.	Buheira	2000	29 days	35%
A/chicken/Egypt/Gharbiya/-15/2017	Broilers	Feb.	Gharbiya	1500	32 days	52%
A/duck/Egypt/Kafr Elshiekh-18/2017	Ducks	May	Kafr El-Sheikh	1500	32 days	29%
A/chicken/Egypt/Buheira-21/2017	Broilers	May	Buheira	2000	30 days	32%

Technical Appendix 1 Table 2. Identity (ID) of the Egyptian HPAIV H5N8 isolated in this study and related viruses with highest identity in the GenBank and GISAID databases

Segment	A/chicken/Egypt/Buheira-12/2017	ID%	A/chicken/Egypt/Gharbiya-15/2017	ID%	A/chicken/Egypt/ Kafr-Elshiekh-18/2017	ID%	A/duck/Egypt /Buheira-21/2017	ID%
PB2	A/duck/Bangladesh/26920/2015 (H3N6)	99.0	A/eurasian_wigeon/Netherlands/ 16015653-001/2016_(H5N8)	99.6	A/peacock/Belgium/1017/ 2017(H5N8)	98.9	A/duck/Bangladesh/26974/ 2015(H3N6)	98.9
PB1	A/domestic_duck/Siberia/ 49_feather/2016 (H6N8)	98.4	A/Eur_Wig/NL-Greonterp/16015653-001/2016 (H5N8)	99.6	A/M_Swan/NL-/16014462-019/2016 (H5N8)	99.7	A/domestic_duck/Siberia/ 49_feather/2016 (H6N8)	98.5
PA	A/Eur_Wig/NL-Greonterp/16015653-001/2016 (H5N8)	98.0	A/Eur_Wig/NL-Greonterp/16015653-001/2016 (H5N8)	99.3	A/Cygnus olor/Belgium/1567/2017(H5N8)	98.6	A/Bar-headed Goose/Qinghai/BTY9-LU/2016 (H5N8)	98.7
HA	A/mute swan/Czech Republic/1296-17_1/2017 (H5N8)	98.9	A/Mallard/Hungary/1574a/2017 (H5N8)	99.1	A/turkey/Poland/83/2016 (H5N8)	98.9	A/mute swan/Czech Republic/1296-17_1/2017 (H5N8)	97.0
NP	A/mallard duck/Netherlands/ 16/2012(H3N2)	97.6	A/mute swan/Kaliningrad/132/2017 (H5N8)	99.7	A/gadwall/Kurgan/2442/ 2016 (A/H5N8)	98.3	(A/mallard duck/Netherlands/18/2012 (H4N2))	97.9
NA	A/Brown-headed Gull/Qinghai/ZTO5-K/2016 (H5N8)	99.1	A/Eur_Wig/NL- /16015653-001/2016 (H5N8)	99.4	A/peacock/Belgium/1017/ 2017(H5N8)	97.3	A/Brown-headed Gull/Qinghai/ZTO6-MU/2016 (H5N8)	98.7
M	A/duck/India/10CA01/2016 (H5N8)	99.7	A/gadwall/Kurgan/2442/2016 (H5N8)	99.2	A/gadwall/Kurgan/2442/ 2016 (A/H5N8)	99.5	A/duck/India/10CA01/2016 (A/H5N8)	99.6
NS	A/duck/India/10CA01/2016 (A/H5N8)	99.3	A/Mallard/Hungary/1574a/2017 (A/H5N8)	99.9	A/goose/Italy/17VIR6358-3/2017 (A/H5N8)	99.4	A/duck/India/10CA01/2016 (A/H5N8)	99.1

HA	Ck12	Ck15	Dk18	CK21	Coot	Teal877	Teal871
Ck12	ID	99.1	99	97.4	98.5	98.5	98.4
Ck15	99.4	ID	99.2	97.1	98.7	98.5	98.4
Dk18	98.7	98.9	ID	97	98.8	98.3	98.2
CK21	97.8	97.7	97	ID	96.7	96.5	96.5
Coot	99.2	99.4	99.1	97.5	ID	99.1	99.1
Teal877	99.6	99.4	98.7	97.8	99.6	ID	99.9
Teal871	99.4	99.2	98.5	97.7	99.4	99.8	ID

PA	Ck12	Ck15	Dk18	CK21	Teal877	Teal871
Ck12	ID	98.1	93.6	94.2	94.3	94.3
Ck15	99.1	ID	92.6	93.2	94.3	94.3
Dk18	96.0	96.3	ID	97.7	94.5	94.5
CK21	97.0	97.3	97.2	ID	95.1	95.1
Teal877	98.0	98.3	96.3	97.6	ID	100.0
Teal871	98.0	98.3	96.3	97.6	100.0	ID

NA	Ck12	Ck15	Dk18	CK21	Coot	Teal877	Teal871
Ck12	ID	98	96.3	98.8	98.7	98.7	98.7
Ck15	97.8	ID	96.6	97.7	99.2	98.5	98.5
Dk18	93.8	95.1	ID	95.8	97.1	96.6	96.6
CK21	97.8	97.2	93.1	ID	98.5	98.3	98.4
Coot	98.0	99.7	95.3	97.4	ID	99.2	99.3
Teal877	97.6	98.7	94.2	96.5	98.9	ID	99.9
Teal871	97.8	98.9	94.4	96.8	99.1	99.7	ID

NP	Ck12	Ck15	Dk18	CK21	Teal877	Teal871
Ck12	ID	97.1	96.5	98.0	94.0	93.9
Ck15	96.9	ID	98.5	97.5	95.2	95.1
Dk18	96.5	99.5	ID	97.0	94.8	94.7
CK21	96.7	98.9	98.5	ID	94.6	94.5
Teal877	96.3	99.3	98.9	98.3	ID	99.9
Teal871	96.1	99.1	98.7	98.1	99.7	ID

PB2	Ck12	Ck15	Dk18	CK21	Teal877	Teal871
Ck12	ID	98.4	98.0	99.3	97.2	97.1
Ck15	98.6	ID	98.6	98.5	97.0	96.9
Dk18	98.4	98.6	ID	98.2	96.9	96.8
CK21	99.0	98.8	98.5	ID	97.1	97.0
Teal877	98.4	98.4	98.1	98.2	ID	99.9
Teal871	98.2	98.2	98.0	98.1	99.8	ID

M1	Ck12	Ck15	Dk18	CK21	Teal877	Teal871
Ck12	ID	98.1	98.8	99.6	99.4	99.4
Ck15	98.4	ID	98.5	98.2	98.1	98.1
Dk18	98.4	98.4	ID	98.6	98.5	98.5
CK21	99.6	98.8	98.8	ID	99.3	99.3
Teal877	99.6	98.0	98.0	99.2	ID	100.0
Teal871	99.6	98.0	98.0	99.2	100.0	ID

PB1	Ck12	Ck15	Dk18	CK21	Teal877	Teal871
Ck12	ID	95.0	95.1	99.5	95.1	95.2
Ck15	98.5	ID	99.4	95.1	98.7	99.0
Dk18	98.8	99.7	ID	95.2	98.9	99.2
CK21	99.4	98.8	99.0	ID	95.2	95.3
Teal877	98.0	98.4	98.6	98.2	ID	99.3
Teal871	98.6	99.0	99.3	98.9	98.8	ID

NS1	Ck12	Ck15	Dk18	CK21	Teal877	Teal871
Ck12	ID	98.6	97.7	99.5	99.1	99.1
Ck15	98.6	ID	99.1	98.2	98.6	98.6
Dk18	97.7	99.1	ID	97.3	97.7	97.7
CK21	99.5	98.2	97.3	ID	98.6	98.6
Teal877	99.1	98.6	97.7	98.6	ID	100
Teal871	99.1	98.6	97.7	98.6	100	ID

Technical Appendix 1 Figure 1. Genetic identity of different genes and proteins of HPAIV H5N8 clade 2.3.4.4 isolated from domestic poultry in Egypt in 2017. Given are the nucleotide and amino acid identity matrices ($^{\text{nucleotide}}\text{ID}_{\text{amino acid}}$) of H5N8 isolated from poultry in this study compared to the wild bird viruses. ID= identical, Ck12= A/chicken/Egypt/Buheira-12/2017, Ck15= A/chicken/Egypt/Gharbiya-15/2017, Dk18= A/chicken/Egypt/Kafr-Elshiekh-18/2017, Ck21= A/duck/Egypt/Buheira-21/2017, Coot= A/Common coot/Egypt/CA285/2016, Teal 877= A/green winged teal/Egypt/877/2016, Teal 871= A/green winged teal/Egypt/871/2016. Only HA and NA gene sequences are available for the common coot virus. Sequences were aligned and identity matrices were calculated using Geneious version 10.

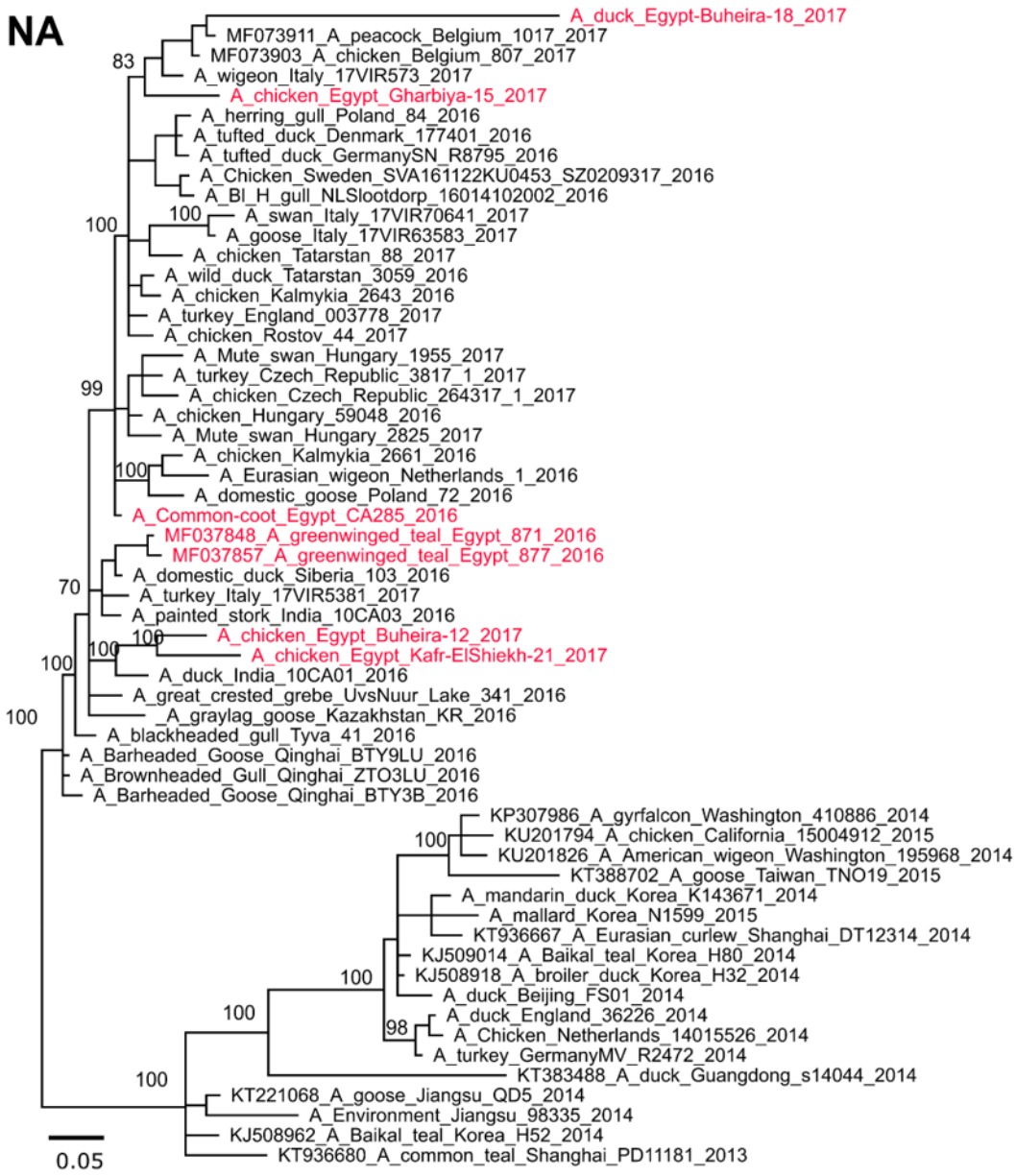

Technical Appendix 1 Figure 2. Phylogenetic relatedness of the NA gene segments of the H5N8 2.3.4.4 viruses from domestic birds in Egypt in 2017. All available sequences of NA of HPAIV H5N8 were retrieved from the GISAID and GenBank databases and aligned using MAFFT. Trees were generated by IQtree and representative viruses were selected for further analysis. Maximum Likelihood mid-point rooted trees were constructed by MrBayes implementing 4 runs, 1000.000 replicates and 10% burn-in using best fit model GTR+G according to BIC value. Egyptian viruses are shown in red.

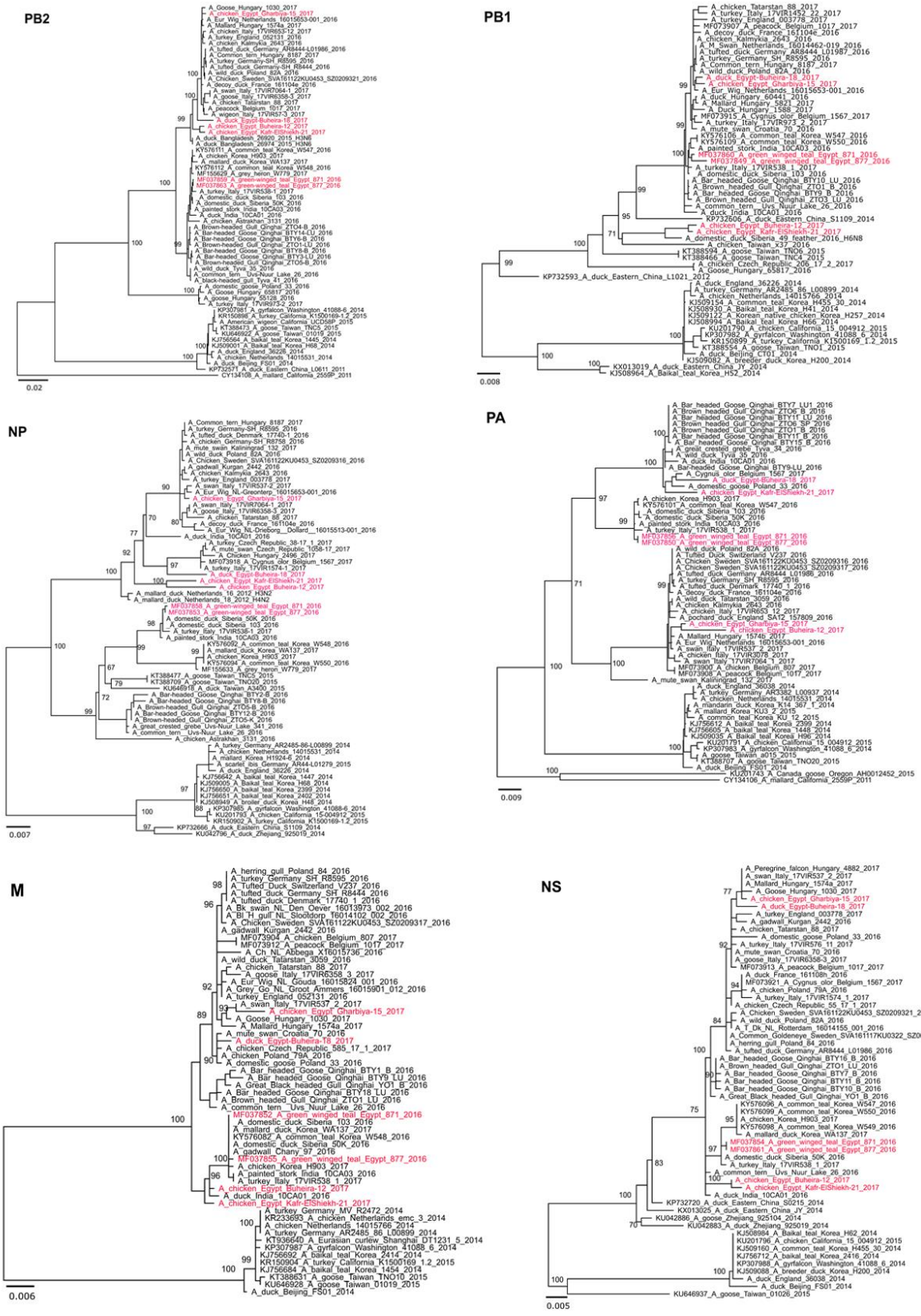
PB2
A_Goose_Hungary_1030_2017
A_chicken_Egypt_Gharbiya-15_2017
A_Eur_Wig_Netherlands_16015653-001_2016
A_Mallard_Hungary_1574a_2017
A_chicken_Italy_17VIR653-12_2017
A_turkey_England_052131_2016
A_chicken_Kalmykia_2643_2016
A_tufted_duck_Germany_AR8444-L01986_2016
A_Common_tern_Hungary_8187_2017
A_turkey_Germany-SH_R8595_2016
A_tufted_duck_Germany-SH_R8444_2016
A_wild_duck_Poland_82A_2016
A_Chicken_Sweden_SVA161122KU0453_SZ0209321_2016
A_decoy_duck_France_161104e_2016
A_swan_Italy_17VIR7064-1_2017
A_goose_Italy_17VIR6358-3_2017
A_chicken_Tatarstan_88_2017
A_peacock_Belgium_1017_2017
A_wigeon_Italy_17VIR57-3_2017
A_duck_Egypt-Buheira-18_2017
A_chicken_Egypt_Buheira-12_2017
A_chicken_Egypt_Kafr-ElShiekh-21_2017
A_duck_Bangladesh_26920_2015_H3N8
A_duck_Bangladesh_26974_2015_H3N8
KY576111_A_common_teal_Korea_W547_2016
A_chicken_Korea_H903_2017
A_mallard_duck_Korea_WA137_2017
KY576112_A_common_teal_Korea_W548_2016
MF156629_A_grey_heron_W779_2017
MF037859_A_green-winged_teal_Egypt_871_2016
MF037863_A_green-winged_teal_Egypt_877_2016
A_turkey_Italy_17VIR538-1_2017
A_domestic_duck_Siberia_103_2016
A_domestic_duck_Siberia_50K_2016
A_painted_stork_India_10CA03_2016
A_duck_India_10CA01_2016
A_chicken_Astrakhan_3131_2016
A_Brown-headed_Gull_Qinghai_ZTO4-B_2016
A_Bar-headed_Goose_Qinghai_BTY14-LU_2016
A_Bar-headed_Goose_Qinghai_BTY6-B_2016
A_Brown-headed_Gull_Qinghai_ZTO1-LU_2016
A_Bar-headed_Goose_Qinghai_BTY8-B_2016
A_Bar-headed_Goose_Qinghai_BTY3-LU_2016
A_Brown-headed_Gull_Qinghai_ZTO5-B_2016
A_wild_duck_Tyva_35_2016
A_common_tern__Uvs-Nuur_Lake_26_2016
A_black-headed_gull_Tyva_41_2016
A_domestic_goose_Poland_33_2016
A_Goose_Hungary_65817_2016
A_goose_Hungary_65128_2016
A_turkey_Italy_17VIR973-2_2017
KP307981_A_gyrfalcon_Washington_41088-6_2014
KR150898_A_turkey_California_K1500169-1-2_2015
A_American_wigeon_California_UCD56P_2015
KT388473_A_goose_Taiwan_TNC5_2015
KU646927_A_goose_Taiwan_01019_2015
KJ756564_A_baikal_teal_Korea_1445_2014
KJ509007_A_Baikal_teal_Korea_H68_2014
A_duck_England_36226_2014
A_chicken_Netherlands_14015531_2014
A_duck_Beijing_FS01_2014
KP732571_A_duck_Eastern_China_L0611_2011
CY134105_A_mallard_California_2559P_2011
0.02
PB1
A_chicken_Tatarstan_88_2017
A_turkey_Italy_17VIR1452_22_2017
A_turkey_England_003778_2017
MF073907_A_peacock_Belgium_1017_2017
A_decoy_duck_France_161104e_2016
A_chicken_Kalmykia_2643_2016
A_M_Swan_Netherlands_16014462-019_2016
A_tufted_duck_Germany_AR8444_L01987_2016
A_turkey_Germany_SH_R8595_2016
A_Common_tern_Hungary_8187_2017
A_wild_duck_Poland_82A_2016
A_duck_Egypt-Buheira-18_2017
A_chicken_Egypt_Gharbiya-15_2017
A_Eur_Wig_Netherlands_16015653-001_2016
A_duck_Hungary_60441_2016
A_Mallard_Hungary_5821_2017
A_Duck_Hungary_1588_2017
MF073915_A_Cygnus_olor_Belgium_1567_2017
A_turkey_Italy_17VIR973_2_2017
A_mute_swan_Croatia_70_2016
KY576106_A_common_teal_Korea_W547_2016
KY576109_A_common_teal_Korea_W550_2016
A_painted_stork_India_10CA03_2016
MF037860_A_green_winged_teal_Egypt_871_2016
MF037849_A_green_winged_teal_Egypt_877_2016
A_turkey_Italy_17VIR538_1_2017
A_domestic_duck_Siberia_103_2016
A_Bar_headed_Goose_Qinghai_BTY10_LU_2016
A_Brown_headed_Gull_Qinghai_ZTO1_B_2016
A_Bar_headed_Goose_Qinghai_BTY9_B_2016
A_Brown_headed_Gull_Qinghai_ZTO3_LU_2016
A_common_tern__Uvs_Nuur_Lake_26_2016
A_duck_India_10CA01_2016
KP732506_A_duck_Eastern_China_S1109_2014
A_chicken_Egypt_Buheira-12_2017
A_chicken_Egypt_Kafr-ElShiekh-21_2017
A_domestic_duck_Siberia_49_feather_2016_H6N8
A_chicken_Taiwan_x37_2016
KT388594_A_goose_Taiwan_TNO5_2015
KT388466_A_goose_Taiwan_TNO1_2015
A_chicken_Czech_Republic_206_17_2_2017
A_Goose_Hungary_65817_2016
KP732593_A_duck_Eastern_China_L1021_2012
A_duck_England_36226_2014
A_turkey_Germany_AR2485_86_L00899_2014
A_chicken_Netherlands_14015766_2014
KJ509154_A_common_teal_Korea_H455_30_2014
KJ508930_A_Baikal_teal_Korea_H41_2014
KJ509122_A_Korean_native_chicken_Korea_H257_2014
KJ508994_A_Baikal_teal_Korea_H66_2014
KU201790_A_chicken_California_15_004912_2015
KP307982_A_gyrfalcon_Washington_41088_6_2014
KR150899_A_turkey_California_K1500169_1-2_2015
KT388554_A_goose_Taiwan_TNO1_2015
A_duck_Beijing_CT01_2014
KJ509082_A_breeder_duck_Korea_H200_2014
KX013019_A_duck_Eastern_China_JY_2014
KJ508964_A_Baikal_teal_Korea_H52_2014
0.008
NP
A_Common_tern_Hungary_8187_2017
A_turkey_Germany-SH_R8595_2016
A_tufted_duck_Denmark_17740-1_2016
A_chicken_Germany-SH_R8758_2016
A_mute_swan_Kaliningrad_132_2017
A_wild_duck_Poland_82A_2016
A_Chicken_Sweden_SVA161122KU0453_SZ0209316_2016
A_gadwall_Kurgan_2442_2016
A_chicken_Kalmykia_2643_2016
A_turkey_England_003778_2017
A_swan_Italy_17VIR537-2_2017
A_Eur_Wig_NL-Greonterp_16015653-001_2016
A_chicken_Egypt_Gharbiya-15_2017
A_swan_Italy_17VIR7064-1_2017
A_goose_Italy_17VIR6358-3_2017
A_chicken_Tatarstan_88_2017
A_decoy_duck_France_161104e_2016
A_Eur_Wig_NL-OrieBorg__Dollard__16015513-001_2016
A_duck_India_10CA01_2016
A_turkey_Czech_Republic_38-17_1_2017
A_mute_swan_Czech_Republic_1058-17_2017
A_Chicken_Hungary_2496_2017
MF073918_A_Cygnus_olor_Belgium_1567_2017
A_turkey_Italy_17VIR1574-1_2017
A_duck_Egypt-Buheira-18_2017
A_chicken_Egypt_Kafr-ElShiekh-21_2017
A_chicken_Egypt_Buheira-12_2017
A_mallard_duck_Netherlands_16_2012_H3N2
A_mallard_duck_Netherlands_18_2012_H4N2
MF037858_A_green-winged_teal_Egypt_871_2016
MF037853_A_green-winged_teal_Egypt_877_2016
A_domestic_duck_Siberia_50K_2016
A_domestic_duck_Siberia_103_2016
A_turkey_Italy_17VIR538-1_2017
A_painted_stork_India_10CA03_2016
KY576092_A_common_teal_Korea_W548_2016
A_mallard_duck_Korea_WA137_2017
A_chicken_Korea_H903_2017
KY576094_A_common_teal_Korea_W550_2016
MF156633_A_grey_heron_W779_2017
KT388477_A_goose_Taiwan_TNC5_2015
KT388709_A_goose_Taiwan_TNO20_2015
KU646918_A_duck_Taiwan_A3450_2015
A_Bar-headed_Goose_Qinghai_BTY2-B_2016
A_Bar-headed_Goose_Qinghai_BTY8-B_2016
A_Brown-headed_Gull_Qinghai_ZTO5-B_2016
A_Bar-headed_Goose_Qinghai_BTY12-B_2016
A_Brown-headed_Gull_Qinghai_ZTO5-K_2016
A_great_crested_grebe_Uvs-Nuur_Lake_341_2016
A_common_tern__Uvs-Nuur_Lake_26_2016
A_chicken_Astrakhan_3131_2016
A_turkey_Germany_AR2485-86-L00899_2014
A_chicken_Netherlands_14015531_2014
A_mallard_Korea_H1924-6_2014
A_scarlet_ibis_Germany_AR44-L01279_2015
A_duck_England_36226_2014
KJ756642_A_baikal_teal_Korea_1447_2014
KJ509005_A_Baikal_teal_Korea_H68_2014
KJ756650_A_baikal_teal_Korea_2399_2014
KJ756651_A_baikal_teal_Korea_2402_2014
KJ508949_A_broiler_duck_Korea_H48_2014
KP307985_A_gyrfalcon_Washington_41088-6_2014
KU201793_A_chicken_California_15-004912_2015
KR150902_A_turkey_California_K1500169-1-2_2015
KP732666_A_duck_Eastern_China_S1109_2014
KU042796_A_duck_Zhejiang_925019_2014
0.007
PA
A_Bar_headed_Goose_Qinghai_BTY7_LU1_2016
A_Brown_headed_Gull_Qinghai_ZTO6_B_2016
A_Bar_headed_Goose_Qinghai_BTY11_LU_2016
A_Brown_headed_Gull_Qinghai_ZTO6_SP_2016
A_Brown_headed_Gull_Qinghai_ZTO1_B_2016
A_Bar_headed_Goose_Qinghai_BTY11_B_2016
A_Bar_headed_Goose_Qinghai_BTY15_B_2016
A_great_crested_grebe_Tyva_34_2016
A_wild_duck_Tyva_35_2016
A_duck_India_10CA01_2016
A_Bar-headed_Goose_Qinghai_BTY9-LU_2016
A_Cygnus_olor_Belgium_1567_2017
A_duck_Egypt-Buheira-18_2017
A_domestic_goose_Poland_33_2016
A_chicken_Egypt_Kafr-ElShiekh-21_2017
A_chicken_Korea_H903_2017
KY576101_A_common_teal_Korea_W547_2016
A_domestic_duck_Siberia_103_2016
A_domestic_duck_Siberia_50K_2016
A_painted_stork_India_10CA03_2016
A_turkey_Italy_17VIR538_1_2017
MF037858_A_green_winged_teal_Egypt_871_2016
MF037850_A_green_winged_teal_Egypt_877_2016
A_wild_duck_Poland_82A_2016
A_Tufted_Duck_Switzerland_V237_2016
A_Chicken_Sweden_SVA161122KU0453_SZ0209316_2016
A_Chicken_Sweden_SVA161122KU0453_SZ0209317_2016
A_tufted_duck_Germany_AR8444_L01986_2016
A_turkey_Germany_SH_R8595_2016
A_tufted_duck_Denmark_17740_1_2016
A_decoy_duck_France_161104e_2016
A_chicken_Kalmykia_2643_2016
A_chicken_Italy_17VIR653_12_2017
A_pochard_duck_England_SA12_157809_2016
A_chicken_Egypt_Gharbiya-15_2017
A_chicken_Egypt_Buheira-12_2017
A_Mallard_Hungary_15746_2017
A_Eur_Wig_Netherlands_16015653-001_2016
A_swan_Italy_17VIR537_2_2017
A_chicken_Italy_17VIR2078_2017
A_swan_Italy_17VIR7064_1_2017
MF073900_A_chicken_Belgium_807_2017
MF073908_A_peacock_Belgium_1017_2017
A_mute_swan_Kaliningrad_132_2017
A_duck_England_36038_2014
A_turkey_Germany_AR3382_L00937_2014
A_chicken_Netherlands_14015531_2014
A_mandarin_duck_Korea_K14_367_1_2014
A_mallard_Korea_KU2_2_2015
A_common_teal_Korea_KU_12_2015
KJ756612_A_baikal_teal_Korea_2399_2014
KJ756605_A_baikal_teal_Korea_1448_2014
KJ509035_A_Baikal_teal_Korea_H96_2014
KU201791_A_chicken_California_15_004912_2015
KP307983_A_gyrfalcon_Washington_41088_6_2014
A_goose_Taiwan_s015_2015
KT388707_A_goose_Taiwan_TNO20_2015
A_duck_Beijing_FS01_2014
KU201743_A_Canada_goose_Oregon_AH0012452_2015
CY134106_A_mallard_California_2559P_2011
0.009
M
A_herring_gull_Poland_84_2016
A_turkey_Germany_SH_R8595_2016
A_Tufted_Duck_Switzerland_V237_2016
A_tufted_duck_Germany_SH_R8444_2016
A_tufted_duck_Denmark_17740_1_2016
A_Bk_swan_NL_Den_Oever_16013973_002_2016
A_Bl_H_gull_NL_Slootdorp_16014102_002_2016
A_Chicken_Sweden_SVA161122KU0453_SZ0209317_2016
A_gadwall_Kurgan_2442_2016
MF073904_A_chicken_Belgium_807_2017
MF073912_A_peacock_Belgium_1017_2017
A_Ch_NL_Abbega_X16015736_2016
A_wild_duck_Tatarstan_3059_2016
A_chicken_Tatarstan_88_2017
A_goose_Italy_17VIR6358_3_2017
A_Eur_Wig_NL_Gouda_16015824_001_2016
A_Grey_Go_NL_Groot_Ammers_16015901_012_2016
A_turkey_England_052131_2016
A_swan_Italy_17VIR537_2_2017
A_chicken_Egypt_Gharbiya-15_2017
A_Goose_Hungary_1030_2017
A_Mallard_Hungary_1574a_2017
A_mute_swan_Croatia_70_2016
A_duck_Egypt-Buheira-18_2017
A_chicken_Czech_Republic_585_17_1_2017
A_chicken_Poland_79A_2016
A_domestic_goose_Poland_33_2016
A_Bar_headed_Goose_Qinghai_BTY1_B_2016
A_Bar_headed_Goose_Qinghai_BTY9_LU_2016
A_Great_Black_headed_Gull_Qinghai_YO1_B_2016
A_Bar_headed_Goose_Qinghai_BTY18_LU_2016
A_Brown_headed_Gull_Qinghai_ZTO1_LU_2016
A_common_tern__Uvs_Nuur_Lake_26_2016
MF037852_A_green_winged_teal_Egypt_871_2016
A_domestic_duck_Siberia_103_2016
A_mallard_duck_Korea_WA137_2017
KY576082_A_common_teal_Korea_W548_2016
A_domestic_duck_Siberia_50K_2016
A_gadwall_Chany_97_2016
MF037855_A_green_winged_teal_Egypt_877_2016
A_chicken_Korea_H903_2017
A_painted_stork_India_10CA03_2016
A_turkey_Italy_17VIR538_1_2017
A_chicken_Egypt_Buheira-12_2017
A_duck_India_10CA01_2016
A_chicken_Egypt_Kafr-ElShiekh-21_2017
A_turkey_Germany_MV_R2472_2014
KP233693_A_chicken_Netherlands_emc_3_2014
A_chicken_Netherlands_14015766_2014
A_turkey_Germany_AR2485_86_L00899_2014
KT936640_A_Eurasian_curlew_Shanghai_DT1231_5_2014
KP307987_A_gyrfalcon_Washington_41088_6_2014
KJ756692_A_baikal_teal_Korea_2414_2014
KR150904_A_turkey_California_K1500169_1-2_2015
KJ756684_A_baikal_teal_Korea_1454_2014
KT388631_A_goose_Taiwan_TNO10_2015
KU646928_A_goose_Taiwan_01019_2015
A_duck_Beijing_FS01_2014
0.006
NS
A_Peregrine_falcon_Hungary_4882_2017
A_swan_Italy_17VIR537_2_2017
A_Mallard_Hungary_1574a_2017
A_Goose_Hungary_1030_2017
A_chicken_Egypt_Gharbiya-15_2017
A_duck_Egypt-Buheira-18_2017
A_turkey_England_003778_2017
A_gadwall_Kurgan_2442_2016
A_chicken_Tatarstan_88_2017
A_domestic_goose_Poland_33_2016
A_turkey_Italy_17VIR576_11_2017
A_mute_swan_Croatia_70_2016
A_goose_Italy_17VIR6358_3_2017
MF073913_A_peacock_Belgium_1017_2017
A_duck_France_161108h_2016
MF073921_A_Cygnus_olor_Belgium_1567_2017
A_chicken_Poland_79A_2016
A_turkey_Italy_17VIR1574_1_2017
A_chicken_Czech_Republic_55_17_1_2017
A_Chicken_Sweden_SVA161122KU0453_SZ0209321_2016
A_wild_duck_Poland_82A_2016
A_T_Dk_NL_Rotterdam_16014155_001_2016
A_Common_Goldeneye_Sweden_SVA161117KU0322_SZ0002165_2016
A_herring_gull_Poland_84_2016
A_tufted_duck_Germany_AR8444_L01986_2016
A_Bar_headed_Goose_Qinghai_BTY16_B_2016
A_Brown_headed_Gull_Qinghai_ZTO1_LU_2016
A_Bar_headed_Goose_Qinghai_BTY7_B_2016
A_Bar_headed_Goose_Qinghai_BTY11_B_2016
A_Bar_headed_Goose_Qinghai_BTY10_B_2016
A_Great_Black_headed_Gull_Qinghai_YO1_B_2016
KY576096_A_common_teal_Korea_W547_2016
KY576099_A_common_teal_Korea_W550_2016
A_chicken_Korea_H903_2017
KY576098_A_common_teal_Korea_W549_2016
A_mallard_duck_Korea_WA137_2017
MF037854_A_green_winged_teal_Egypt_871_2016
MF037861_A_green_winged_teal_Egypt_877_2016
A_domestic_duck_Siberia_50K_2016
A_turkey_Italy_17VIR538_1_2017
A_common_tern__Uvs_Nuur_Lake_26_2016
A_chicken_Egypt_Buheira-12_2017
A_chicken_Egypt_Kafr-ElShiekh-21_2017
A_duck_India_10CA01_2016
KP732720_A_duck_Eastern_China_S0215_2014
KX013025_A_duck_Eastern_China_JY_2014
KU042886_A_goose_Zhejang_925104_2014
KU042883_A_duck_Zhejiang_925019_2014
KJ508984_A_Baikal_teal_Korea_H62_2014
KU201796_A_chicken_California_15_004912_2015
KJ509160_A_common_teal_Korea_H455_30_2014
KJ756712_A_baikal_teal_Korea_2416_2014
KP307988_A_gyrfalcon_Washington_41088_6_2014
KJ509088_A_breeder_duck_Korea_H200_2014
A_duck_England_36038_2014
A_duck_Beijing_FS01_2014
KU646937_A_goose_Taiwan_01026_2015
0.005

Technical Appendix 1 Figure 3. Phylogenetic relatedness of non-HA/NA gene segments of the H5N8 2.3.4.4 viruses from domestic birds in Egypt in 2017. All available sequences of H5N8 viruses were retrieved from the GISAID and GenBank databases. First tree was generated by IQtree and representative viruses were selected for further analysis. Maximum Likelihood mid-point rooted trees were generated by MrBayes using 4 runs each of 1000.000 replicates and 10% burn-in after selection of the best fit model GTR+G according to BIC value as implemented in Topali v2. All trees were edited and prepared for publishing using FigTree and Inkscape.